Electrocoagulation-flotation treatment followed by sedimentation of carpet cleaning wastewater: optimization of key operating parameters via RSM-CCD

Elena Shakeri[a,b,†], Milad Mousazadeh[a,b,†], Hedieh Ahmadpari[c], Işık Kabdaşlı[d], Hamzeh Ali Jamali[e], Nuno S.Graça[f], Mohammad Mahdi Emamjomeh[e,*]

[a]*Student Research Committee, Qazvin University of Medical Sciences, Qazvin, Iran, emails: shakeri.elena@yahoo.com (E. Shakeri), m.milad199393@gmail.com (M. Mousazadeh)*
[b]*Department of Environmental Health Engineering, School of Health, Qazvin University of Medical Sciences, Qazvin, Iran*
[c]*Department of Irrigation and Drainage, College of Aburaihan, University of Tehran, Iran, email: h.ahmadpari@gmail.com*
[d]*İstanbul Technical University, Civil Engineering Faculty, Environmental Engineering Department, Ayazağa Campus, 34469 Maslak, İstanbul, Republic of Turkey, email: kabdasli@itu.edu.tr*
[e]*Social Determinants of Health Research Center, Research Institute for Prevention of Non-Communicable Diseases, Qazvin University of Medical Sciences, Qazvin, Iran, emails: jamalisadraei@gmail.com (H. Ali Jamali), m_emamjomeh@yahoo.com (M.M. Emamjomeh)*
[f]*Laboratory of Separation and Reaction Engineering – Laboratory of Catalysis and Materials (LSRE-LCM), Department of Chemical Engineering, University of Porto, Rua Dr. Roberto Frias, s/n, 4200-465 Porto, Portugal, email: nunopsg@fe.up.pt*

ABSTRACT

In the present study, the treatment of carpet cleaning wastewater was optimized for electrocoagulation-flotation (ECF) followed sedimentation. In the experimental study, an ECF reactor equipped with four monopolar, parallel-connected aluminum electrodes was utilized. For the optimization, the process variables were selected as methylene blue active substance (MBAS), chemical oxygen demand (COD), and turbidity removal efficiencies, along with the characterization of sludge settling volume at 60 min (SSV_{60}). For this goal, response surface methodology (RSM) under central composite design (CCD) was employed to optimize the critical factors viz. pH (3.64–10.36), current intensity (0.66–2.34 A), and electrolysis time (9.55–110.45 min). RSM-CCD optimized these key factors to achieve maximum removal efficiencies and minimize SSV_{60}. Based on the RSM-CCD prediction, the optimum operating conditions were as pH of 5.1, the current intensity of 2 A, and electrolysis time of 53.5 min, in which the obtained model predicted 83.56%, 82.54%, 88.14%, and 226.22 mL/L for MBAS, COD, turbidity, and SSV_{60}. Correspondingly, the predictions were in agreement with the actual results (85.50%, 84.35%, 90.50%, and 240.17 mL/L, respectively). The operating cost in the optimal conditions was calculated as 0.673 USD/m³. The results of the study indicated that the electrocoagulation-flotation followed sedimentation was a cost-effective treatment process in removing target pollutants from the carpet cleaning wastewater.

Keywords: Electrocoagulation-flotation; Carpet cleaning wastewater; Aluminum electrodes; Optimization; Sludge settling volume

1. Introduction

Every year in the world, the carpet cleaning industry, for its various processes, uses a large amount of water. According to a study conducted in Iran, about 30 L of water per square meter is used in various carpet cleaning [1]. Wastewater from washing industries such as laundry, carpet cleaning, and car wash offers combinations of different levels, including suspended solids, turbidity, chemical oxygen demand (COD), and surfactants. Surfactants,

* Corresponding author.

[†]These authors contributed equally to this work.

meanwhile, are emerging pollutants that are constantly entering the environment through wastewater, causing profound effects on the environment [2,3]. Methylene blue active substances (MBAS), as an anionic surfactant, account for about 60% of the world's surfactant production [4]. Given that a significant amount of wastewater is generated annually from the carpet cleaning wastewater (CCW), as well as the production of hazardous compounds from it, therefore, it is important to handle this wastewater before discharging it into the environment.

Various treatment methods such as advanced oxidation process [5], adsorption [6], coagulation [7], biological [8,9], and membrane filtration [10] have been suggested from time to time. But above-mentioned technologies have several drawbacks such as long process time, high energy consumption, membrane fouling, inefficient treatment, and sludge disposal problem, which make these treatment systems less attractive from the sustainability point of view, failing to provide processes with low-carbon, low energy consumption, expensive capital investment. In terms of technological viability economics, and public needs, the emphasis on wastewater management has recently moved from pollution control to resource reutilization. Among them, electrocoagulation-flotation (ECF) as an affordable technology offers potential advantages such as environmentally friendly operation, low capital cost, and has no requirement of chemical constituents of the wastewater [11–13]. The ECF is a chemical treatment process that involves the following steps: (i) formation of metal hydroxide flocs in solution by electro-dissolution of the sacrificial anodes, (ii) formation of coagulants in the aqueous phase, and (iii) adsorption of contaminants on coagulants, resulting in removal via sedimentation/flotation [14–16]. In the last decade, ECF is used in the treatment of various types of water and wastewater such as textile [17,18], waste off-set printing [19], urban [20], waste fountain solution [21], phosphate industrial [22], industrial park [23], laundry [24], automotive service station [25], domestic wastewater and carwash [26].

Response surface methodology (RSM) is a collection of statistical and mathematical techniques used to optimize the process parameters and their interactions with a minimum number of experiments to produce statistically significant results [27,28]. The characteristic of RSM is that it can only be defined as numerical parameters (e.g., initial pH), and it is not useful for parameters that are verbal (e.g., electrode material). Many researchers have used this method to optimize process parameters for the removal of various contaminants by ECF [29–32]. For instance, Khorram and Fallah [33] found 40% COD removal and 98% dye decolorization from textile industrial wastewater by EC under the optimized process parameters via RSM: pH of 5.5, the current density of 15 mA/cm², and EC time of 23 min. Another study showed that linear alkylbenzene sulfonate, and phenol of 96.7%, and 87.65% removals were achieved using ECF followed with filtration under RSM optimized process conditions (initial pH of 7.5, current value of 1.72 A, and electrolysis time of 90 min), respectively [25]. One of the inherent features of the ECF process is the production of sludge after the treatment process. Since sludge dewatering is an essential and costly part of the wastewater treatment process, the sludge

separation method by the settled process is considered to be cost-effective and popular. Thus, the characterization of settled sludge volume (SSV) is one of the important parameters in the assessment of the efficacy of the ECF process. In practice, ECF followed by sedimentation is the most common choice.

Based on our literature survey, no reports have been devoted to the application of ECF treatment of CCW using RSM optimization, and this gap of knowledge is obvious in the above-mentioned treatment process. In this context, the current work aims the removal of MBAS, COD, and turbidity, and characterize SSV_{60} from CCW using an aluminum-based ECF unit followed by a settling step. In order to attain maximum removal efficiencies and minimum SSV, RSM under central composite design (CCD) was used to optimize and investigate the effect of the three process parameters as independent variables, including pH, current intensity, and electrolysis time on target responses.

2. Brief description of the EC process

EC water treatment can be achieved through the destabilization of suspensions, entrapment of particles, and adsorption of dissolved contaminants. Applying an electric current into the aqueous medium causes the electrolytic oxidation of sacrificial anodes to release metal coagulants into the solution, and at the cathode, hydrogen gas is produced in the form of bubbles. The basic unit of EC involves an electrolytic chamber with an anode and cathode connected externally to a DC power supply and dipped in the solution to be treated. The most common electrode materials are iron and aluminum. However, aluminum electrodes are preferred over iron electrodes due to easy availability and reliability [34]. The chemical reactions in EC reactors using aluminum electrodes are as follows:

Aluminum anode:

$$Al_{(s)} \rightarrow Al_{(aq)}^{3+} + 3e^- \tag{1}$$

At cathode:

$$2H_2O + 2e^- \rightarrow 2OH^- + H_2(g) \; (\text{alkaline condition}) \tag{2}$$

$$2H_2O + 2e^- \rightarrow 2H_2O + H_2 \; (\text{acidic condition}) \tag{3}$$

In bulk solution:

$$Al^{3+} + H_2O \rightleftharpoons Al(OH)^{2+} + H^+ \tag{4}$$

$$Al(OH)^{2+} + H_2O \rightleftharpoons Al(OH)_2^+ + H^+ \tag{5}$$

$$Al(OH)_2^+ + H_2O \rightleftharpoons Al(OH)_3^0 + H^+ \tag{6}$$

$$\text{Al}(\text{OH})_3^0 + \text{H}_2\text{O} \rightleftharpoons \text{Al}(\text{OH})_4^- + \text{H}^+ \tag{7}$$
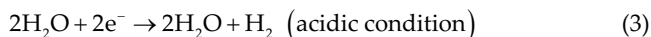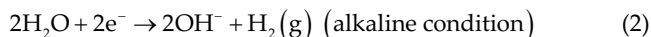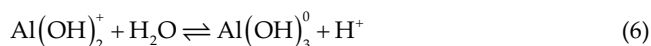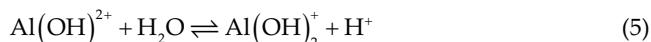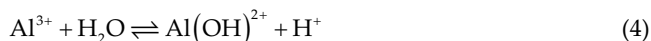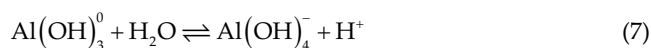
Water dissociation reaction:

$$\text{H}_2\text{O} \rightleftharpoons \text{H}^+ + \text{OH}^- \tag{8}$$

Using aluminum as the electrode material, the anodes produce Al^{3+} ions. These cations immediately undergo additional reactions forming various kinds of monomeric and polymeric species, such as $\text{Al}_2(\text{OH})^{2+}$, $\text{Al}_2(\text{OH})_2^{4+}$, $\text{Al}_7(\text{OH})_{17}^{4+}$, and $\text{Al}_{13}\text{O}_4(\text{OH})_{24}^{7+}$, based on the solution pH. Eventually, these species convert to $\text{Al}(\text{OH})_{3(s)}$ due to the complex precipitation kinetics [35].

3. Experimental

3.1. Carpet cleaning wastewater

The wastewater samples were collected from a carpet cleaning plant located in Qazvin, Iran. The characterization of the samples used in our experimental study is given in Table 1. Zazouli et al. [36] reported the characteristics of the hospital laundry wastewater as COD, and surfactant in the range of 650–1,080 mg/L, and 3.19–6.48 mg/L, respectively. Changani et al. [1] also observed that the average level of the effluent characteristics of the carpet cleaning industry were COD of 367.4 mg/L, and detergent of 55.51 mg/L. Furthermore, COD, MBAS, turbidity, pH, and electrical conductivity were detected as 229–1,446 mg/L, 25–353 mg/L, 137–2,250 NTU, 7.7–8.2, and 250–1,890 μs/cm, respectively, in car wash wastewater [26]. As seen from Table 1, concentrations of all pollutants measured in the present study were within the range reported in the relevant literature.

The effluent analyses were performed on a sample withdrawn from the supernatant. COD was analyzed using a digestion reactor (LT200, Hach, USA) and spectrophotometer (DR 6000 UV-Vis, Hach, Germany) at 620 nm according to Standard test Methods for the Examination of Water and Wastewater: 5220D (closed reflux colorimetric) [37]. MBAS was measured with a spectrophotometric (DR 6000 UV-Vis, Hach, Germany) according to the method suggested by Chitikela et al. [38]. SSV was measured according to the standard method [37]. Nephelometric Method [39] was used for the analysis of turbidity by spectrophotometer (2100 AN, Hach, Germany). The MBAS, COD, and turbidity removal efficiency (R) (%) was calculated as Eq. (9) [40]:

Table 1
Wastewater characterization of carpet cleaning

Parameter	Concentration
COD, mg/L	670–677
Turbidity, NTU	118–126
MBAS, mg/L	19.7–21
Conductivity, mS/m	0.89–0.90
pH	9.1–9.3

$$\text{Removal efficiency}(\%) = \frac{(A_0 - A_t)}{A_0} \times 100 \tag{9}$$

where A_0 is initial and A_t is final pollutant concentration (mg/L).

3.2. Set up a treatment system

The ECF unit is a 500 mL effective capacity cylindrical reactor made of glass. The reactor is equipped with four monopolar, parallel-connected aluminum electrodes. The electrodes dimensions were 60 mm (width) × 100 mm (length) × 2 mm (depth) and vertically placed in the center of the reactor. The distance between the electrodes was fixed at 2 mm. A DC power supply (model JPS303D, Iran; E_{max}: 30V) was connected to the electrode supply to offer an appropriate voltage and current. After each run, the electrodes were well rubbed with abrasive paper in order to prevent electrode passivation and then rinsed with the combination of acid reagent and distilled water to eradicate any solid residues on the surfaces. A magnetic stirrer (model SHA R-50, Iran) was placed at the bottom of the reactor to ensure homogenous mixing at a constant rate of 250 rpm during all ECF runs. The ECF set-up is depicted in Fig. 1.

3.3. Experimental procedure

The initial pH of the samples was adjusted to the desired value using either H_2SO_4 (0.1 N) or NaOH (0.1 N) solution. After pH adjustment, the electrical conductivity of samples was recorded. In order to increase the conductivity to achieve electrochemical ion transfer, sodium chloride (NaCl) was added to the wastewater sample during the ECF process to provide the specified electrical current. Then, the sample was poured into the reactor, and current and voltage were adjusted on the DC power supply to the desired value of current intensity. After that, an ECF trial was initiated. At the end of each ECF run, the reactor content was allowed to settle. At the end of the settling time of 60 min, SSV values were recorded, and concurrently the samples were withdrawn from the supernatants for the analyses of COD, MBAS, and turbidity. All the ECF runs were performed in duplicate, and their arithmetic averages were reported.

3.4. Operation cost

The electrode mass lost and the energy consumed is the major cost items that contributed to the operation cost of the ECF process [25]. The operation cost can be calculated by the following general Eq. (10):

$$\text{Operation cost} = \alpha C_{\text{electrode}} + \beta C_{\text{energy}} \tag{10}$$

where $C_{\text{electrode}}$ and C_{energy} are electrode material consuming and energy requirement for pollutant removal, respectively. α and β are the price of 1 kWh electricity (0.08 USD/kWh by Iranian Energy Ministry) and the price of electrode material (1.95 USD/kg of Al by the Iranian markets in 2020) [25].
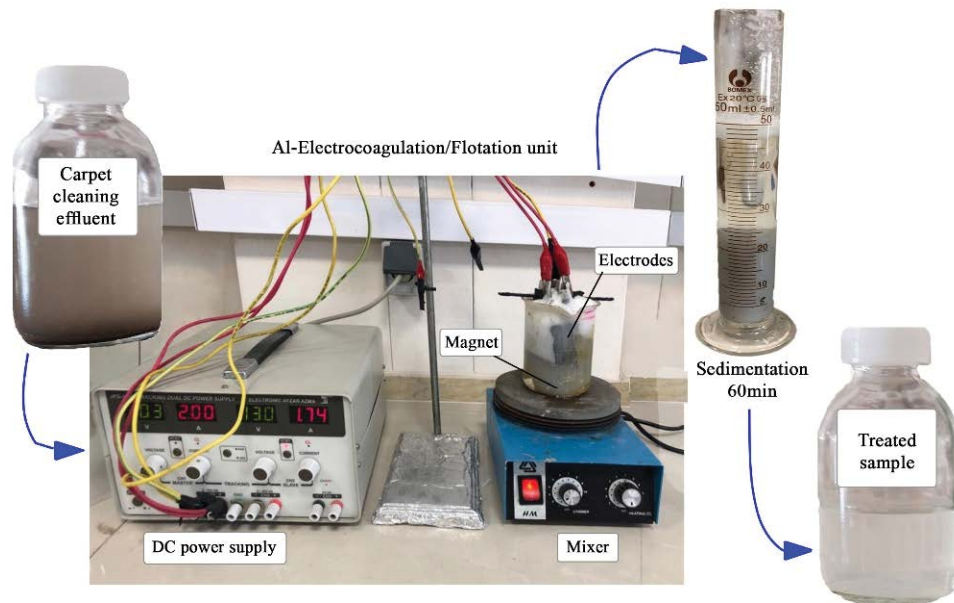
Fig. 1. Original apparatus of the electrocoagulation-flotation-sedimentation laboratory-scale treatment system.

The electrical energy consumption can be calculated by Eq. (11), and Faraday's law is used for calculating electrodes cost, which alters according to the current intensity and electrolysis time as Eq. (12) [25]:

$$C_{energy}\left(\frac{kWh}{m^3}\right) = \frac{U \times I \times T}{V_L} \quad (11)$$

$$C_{electrode}\left(\frac{kgAl}{m^3}\right) = \frac{I \times T \times MV}{Z \times F \times V_L} \quad (12)$$

where U, I, T, and V_L are the cell voltage (V), current intensity (A), time of electrolysis (h), and wastewater volume (m^3), respectively. MV is the molecular mass of Al (26.98 g mol^{-1}), Z is the number of the transferred electrons (=3), and F is the constant of Faraday (96,487 C mol^{-1}).

3.5. Experimental design

One of the common methods used in modeling and analyzing the optimum conditions is the response surface method. RSM leads to reduce the times and the costs of the test [41]. In the RSM model, it is focused on the efficacy and the interactions between the independent variables such as initial pH, current intensity and electrolysis time, and the responses, including MBAS, COD, and turbidity removal efficiency, and SSV. The experimental results of trials were analyzed by Design Expert 7 software using the CCD method. A series of 20 experiments based on three independent variables, including pH, current intensity, and electrolysis time with five levels, were codified to be optimized. The level of independent variables was determined based on the pre-test results and the values presented in the literature [42,43]. Fig. 2 summarizes the flowchart of the steps to

follow for the X value. The coded critical factors (–1.68, –1, 0, +1, +1.68) and the experimental domain are shown in Table 2, which is obtained according to pre-tests. The system behavior was described by second-order polynomial Eq. (13) [44]:

$$y(\%) = \beta_0 + \sum_{i=1}^{k} \beta_i X_i + \sum_{i=1}^{k} \beta_{ii} X_i^2 + \sum_{1 \le i \le j}^{k} \beta_{ij} X_i X_j + \varepsilon \quad (13)$$

where y is the response; i, j, and β_0 are the linear constant, the second-order, and the constant coefficient, respectively. The regression constant, quadratic coefficient, and the interaction coefficient are β_i, β_{ii}, β_{ij} respectively; x_i and x_j are the coded independent variables.

4. Results and discussion

4.1. Response analysis by CCD

Table 3 shows the actual vs. predicted results of MBAS, COD, and turbidity removal efficiencies, as well as SSV$_{60}$ using the ECF-sedimentation process. Based on the obtained data by CCD-RSM, the highest removal efficiencies for MBAS, COD, and turbidity were 95.48%, 94.99%, and 98.75%, respectively, and the highest SSV$_{60}$ was 420.33 mL/L. In the current work, as presented in Table 4, a quadratic model was selected for predicting responses to fit the model.

The analysis of variance (ANOVA) results of the effect of independent variables on targeted responses are presented in Table 5. The data show that there are good fits to the quadratic model with relatively high R^2, especially for MBAS and turbidity removals (0.93 and 0.94, respectively). This has also been approved by the large F-values and the small p-values (<0.05). The lack of fit F-test defines the variation of data around the fitted model. Wherefore, if the model fits the data well, the lack of fit will not be significant. As can be seen in Table 5, lack of fit for the obtained models for
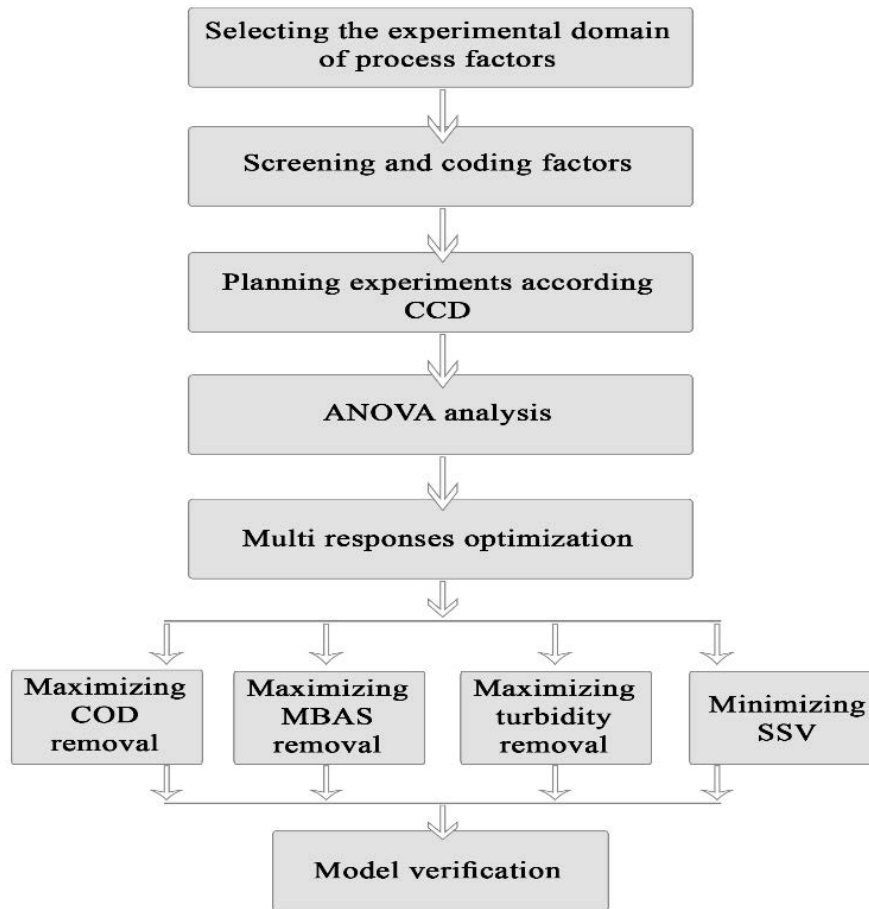
Fig. 2. Flowchart for the optimization of RSM-CCD.

Table 2
Experimental domain of CCD

Independent	Code	Code levels				
Variables	Variables	−1.68	−1	0	+1	+1.68
Initial pH	A	3.64	5	7	9	10.36
Current intensity (A)	B	0.66	1	1.5	2	2.34
Electrolysis time (min)	C	9.55	30	60	90	110.45

all responses were not statistically significant, representing weak noise of the model compared to their signal.

As shown in the result of ANOVA in Table 5, initial pH (A), current intensity (B), electrolysis time (C), the quadratic terms of pH_0 (A^2), and the quadratic terms of electrolysis time (C^2) have substantial effects ($p < 0.05$) on all responses. In addition, two factors of $A \times C$ have significant effects on MBAS, COD, and turbidity removal efficiencies, and two factors of $B \times C$ have significant effects on MBAS removal efficiencies. Furthermore, two factors of $A \times B$ have significant effects on COD, and turbidity removal efficiencies.

Figs. 3 and 4a, b depict the diagnostic plot of actual vs. predicted values for MBAS, COD, turbidity removal, and

SSV_{60}, which attests to the good predictive capacity of the model. The data obtained from the experiments more or less overlap with the predicted data by the model. As can be seen, the points follow an almost straight line, so the model provides a good prediction of MBAS, COD, and turbidity removal efficiencies as well as SSV_{60}.

The results of the significance of factors are confirmed by the Pareto chart depicted in Fig. 5. In the figure, percent contributions (P_i) are defined as the ratio of the pure sum (S_A) of the factors to the total sum of squares (SS) as Eq. (14) [45].

$$P_i\left(\%\right) = \frac{S_A}{SS_T} \tag{14}$$

As can be seen from Fig. 5, the factor of electrolysis time had the highest percentage contribution as 31.81%, 17.48%, and 38.37% for MBAS and COD removal efficiencies and SSV_{60}, respectively. In addition, the current intensity was the most important factor for turbidity removal efficiency as a contribution of 30.58%. While, the factor of initial pH does not influence noticeably on the responses as it contributes to 5.92%, 7.93%, and 7.54%, for MBAS, turbidity, and SSV_{60}, respectively.

Table 3
Design matrix of experiments and results of CCD

| Runs | Experimental matrix | | | Removal efficiency (%) | | | | | | SSV_{60} (mL/L) | |
| | | | | MBAS | | COD | | Turbidity | | | |
	A	B	C	Actual	Predicted	Actual	Predicted	Actual	Predicted	Actual	Predicted
1	1	1	1	90.91	91.67	94.85	91.31	83.25	86.08	400.34	440.06
2	0	0	0	85.86	89.12	87.17	80.38	96.40	91.61	380.56	330.95
3	–1	1	1	74.58	75.95	85.25	83.65	93.57	95.86	310.45	320.63
4	0	0	0	81.72	89.12	75.05	80.38	96.21	91.61	330.33	330.95
5	–1	–1	–1	48.86	49.79	54.26	52.55	64.45	63.42	80.33	50.17
6	0	+1.68	0	92.00	94.18	85.38	88.73	98.75	96.01	400.75	360.25
7	0	0	0	89.48	89.12	74.01	80.38	83.00	91.61	230.33	330.95
8	–1	–1	1	69.10	69.56	50.26	45.57	94.61	96.19	150.35	150.10
9	0	0	0	95.48	89.12	94.99	80.38	98.00	91.61	410.66	330.95
10	0	0	+1.68	91.10	86.01	73.60	77.55	98.40	94.65	420.33	400.88
11	0	0	0	91.86	89.12	73.37	80.38	90.11	91.61	330.33	330.95
12	+1.68	0	0	85.91	80.99	76.43	79.14	67.59	66.30	200.64	190.63
13	0	0	–1.68	49.58	52.29	49.94	53.42	70.44	71.64	80.33	80.99
14	1	1	–1	70.10	71.33	56.20	55.64	91.28	91.50	150.25	160.06
15	–1	1	–1	81.96	76.30	77.43	73.24	76.67	77.41	100.15	120.47
16	0	–1.68	0	84.20	79.63	65.87	69.95	65.00	65.19	130.33	170.03
17	–1.68	0	0	56.29	58.83	52.15	56.87	83.25	82.00	50.13	50.35
18	0	0	0	89.91	89.12	78.99	80.38	85.50	91.61	330.33	330.95
19	1	–1	1	93.53	100.87	90.73	89.66	62.36	63.43	300.25	280.50
20	1	–1	–1	60.10	60.42	75.03	71.38	55.00	54.52	110.35	100.73

Table 4
Quadratic models for predicting responses of CCW using ECF-sedimentation process

Parameters	Equation for real variables
MBAS removal efficiency (%)	$+89.12 + 6.59A + 4.33B + 10.03C + 5.17AC - 5.03BC - 6.79A^2 - 7.06C^2$
COD removal efficiency (%)	$+80.38 + 6.62A + 5.58B + 7.17C - 9.11AB + 6.32AC - 4.38A^2 - 5.27C^2$
Turbidity removal efficiency (%)	$+91.61 - 4.67A + 9.16B + 6.84C + 5.75AB - 5.97AC - 6.17A^2 - 3.89B^2 - 2.99C^2$
SSV_{60} (mL/L)	$+333.62 + 4196A + 56.73B + 94.61C - 75.54A^2 - 31.36C^2$

A: initial pH; B: current intensity; C: electrolysis time.

4.2. MBAS removal efficiency

Fig. 6 delineates the 2D contours (a) and 3D (b) plots for MBAS removal efficiency as a function of current intensity and pH, respectively. As the current intensity and pH of the process increased, the MBAS removal efficiency also increased. The MBAS removal enhanced to highest rate (approximately 93%) when the current intensity increased to 2 A and at pH 8 and remained virtually constant at pH values higher than 8. Al(OH)$_4^-$ as monomeric hydroxo-complex is the dominant species at alkaline pH values. On the other hand, surfactants have Na$^+$ in their hydrophilic head, so charge neutralization is likely to occur at this pH [46]. Nevertheless, at higher current intensity, no significant increase in MBAS removal efficiency was observed. At the acidic pH range between 4 and 6, with increasing current intensity up to 1.5 A, an increase in MBAS removal rate was more evident, which also achieved 80% efficiency.

As seen from Table 6, the results obtained for MBAS removal in the current work are in good agreement with the recent scientific literature [26,46]. Barışçı and Turkay [46] reported that MBAS of domestic greywater treated using electrocoagulation process. They observed highest removal rate (reduced to less than 1 mg/L) of MBAS occurred at initial pH of 7.62 and a current density of 1 mA/cm². Emamjomeh et al. [26] using combined processes of electrocoagulation/flotation, sedimentation, and filtration in the treatment of MBAS from carwash wastewater, stated that 95.2% removal rate of MBAS at pH of 7.67, current of 1.69 A, and time of 90 min. They explained that the MBAS removal rate declined after pH 7 and applied current of 1 A. Dimoglo et al. [47] compared the performances of the

Table 5
ANOVA results of quadratic for MBAS, COD, and turbidity removals, and SSV_{60}

Source of variations	Sum of square				Degree of freedom				Mean square				F-value				p-value Prob. > F			
	R_{MBAS}	R_{COD}	$R_{turbidity}$	SSV_{60}	R_{MBAS}	R_{COD}	$R_{turbidity}$	SSV_{60}	R_{MBAS}	R_{COD}	$R_{turbidity}$	SSV_{60}	R_{MBAS}	R_{COD}	$R_{turbidity}$	SSV_{60}	R_{MBAS}	R_{COD}	$R_{turbidity}$	SSV_{60}
Model	4,020.81	3,481.09	3,504.03	293,100	9	9	9	9	446.76	386.79	389.34	32,565.18	15.16	7.20	15.97	12.71	0.0001^	0.0024^	<0.0001*	0.0002
A-pH$_0$	592.51	598.97	297.55	24,044.41	1	1	1	1	592.51	598.97	297.55	24,044.41	20.10	11.15	12.21	9.38	0.0012^	0.0075^	0.0058	0.0120
B-current intensity	255.56	425.86	1,146.14	43,945.75	1	1	1	1	255.56	425.86	1,146.14	43,945.75	8.67	7.93	47.02	17.15	0.0147^	0.0183^	<0.0001*	0.0020
C-electrolysis time	1,372.88	702.68	638.94	122,300	1	1	1	1	1,372.88	702.68	638.94	122,300	46.58	13.08	26.21	47.70	<0.0001*	0.0047^	0.0005	<0.0001*
AB	121.68	663.75	264.39	199.30	1	1	1	1	121.68	663.75	264.39	199.30	4.13	12.35	10.85	0.078	0.0696	0.0056^	0.0081	0.7860
AC	214.04	319.16	284.77	3,186.81	1	1	1	1	214.04	319.16	284.77	3,186.81	7.26	5.94	11.68	1.24	0.0225^	0.0350^	0.0066	0.2909
BC	202.41	151.12	102.60	5,023.53	1	1	1	1	202.41	151.12	102.60	5,023.53	6.87	2.81	4.21	1.96	0.0256^	0.1245	0.0673	0.1918
A^2	664.85	275.96	549.43	82,232.97	1	1	1	1	664.85	275.96	549.43	82,232.97	22.56	5.14	22.54	32.09	0.0008^	0.0469^	0.0008	0.0002
B^2	8.81	1.96	218.34	9,732.13	1	1	1	1	8.81	1.96	218.34	9,732.13	0.30	0.036	8.96	3.80	0.5966	0.8525	0.0135	0.0799
C^2	718.49	399.77	129.06	14,176.69	1	1	1	1	718.49	399.77	129.06	14,176.69	24.38	7.44	5.29	12.71	0.0006^	0.0213^	0.0442	0.0405
Residual	294.75	537.32	243.77	25,629.21	10	10	10	10	29.47	53.73	24.38	2,562.92								
Lack of fit	180.68	157.99	45.15	6,808.90	5	5	5	5	36.14	31.60	9.03	1,361.78	1.58	0.42	0.23	0.36	0.3130	0.8208	0.9351	0.8556
Pure error	114.07	379.33	198.62	18,820.31	5	5	5	5	22.81	75.87	39.72	3,764.06								
Cor. total	4,315.56	4,018.41	3,747.79	318,700	19	19	19	19												

R_{MBAS} R^2/R^2_{adj} (%) = 0.93/0.87
R_{COD} R^2/R^2_{adj} (%) = 0.87/0.75
$R_{turbidity}$ R^2/R^2_{adj} (%) = 0.94/0.88
SSV_{60} R^2/R^2_{adj} (%) = 0.92/0.85

*Highly significant
^Significant

Fig. 3. Comparison of predicted and actual responses: (a) MBAS removal and (b) COD removal.
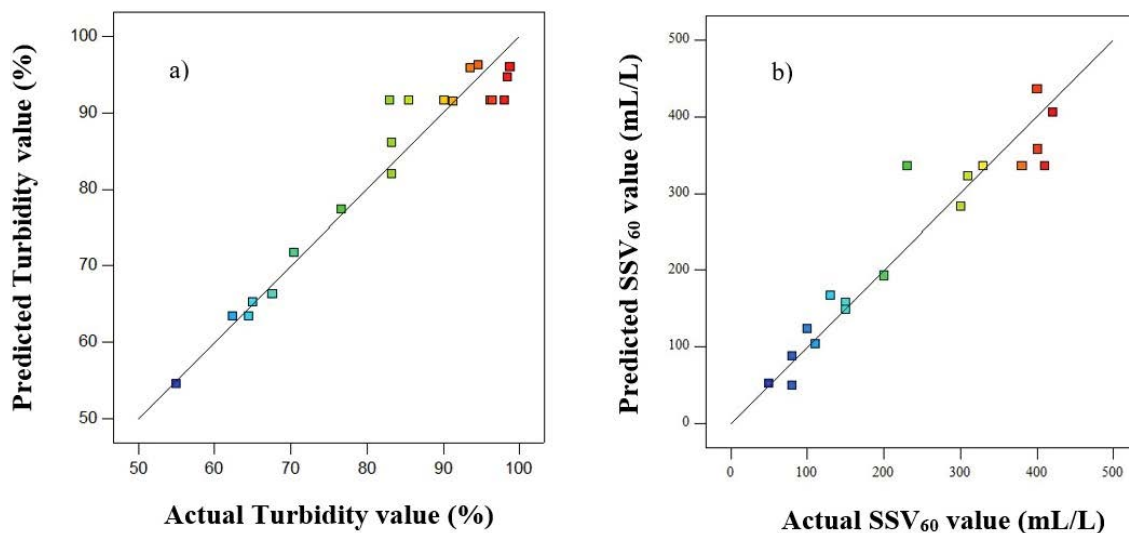
Fig. 4. Comparison of predicted and actual responses: (a) turbidity removal and (b) SSV_{60}.

pilot plant and lab-scale of EC and EF treatment for the laundry effluent. They demonstrated that MBAS removals of 80%–85% were achieved at an initial pH of 5.5 in 7 min during pilot-scale operation, and 97% MBAS removal could be obtained within 5 min at initial pH of 5. In contrast with our work, Mohebrad et al. [48] reported that 90.39% anionic surfactant removal efficiency could be achieved by using electrocoagulation/flotation process using aluminum electrode at pH 3 and reaction time of 90 min.

4.3. COD removal efficiency

Figs. 7a and b exhibit the interaction of electrolysis time and pH in the COD removal efficiency; as seen from the figure, efficiency improved with the increases of electrolysis time and initial pH. At the initial electrolysis time and current intensity of 1.5 A, with increasing pH, the COD removal rate is improved slightly and then decreases. A partial

decline arose in COD removal efficiency after pH 8 at the low level of electrolysis time. The highest COD removal efficiency (94.99%) was achieved within 60 min and at pH of 7 and current intensity of 1.5 A. At extended electrolysis times from 60 to 90 min, there was a gradual increase in the COD removal efficiency as pH shifted to a slightly alkaline pH value of 8. It was evident that the number of aluminum ions released by the sacrificial anode increased with increasing electrolysis time [53]. On the other hand, more hydrogen bubbles were produced at the cathode surface by increasing time, which not only improved the degree of mixing but could also enhance the flotation ability of the ECF cell, which in turn increased COD removal efficiency.

The COD removal efficiencies obtained from the present study found to be comparable with the literature value given in Table 6. Janpoor et al. [24] explored the treatment of laundry wastewater (with COD of 4,155 mg/L) by electrocoagulation with aluminum. Their results indicated that initial COD
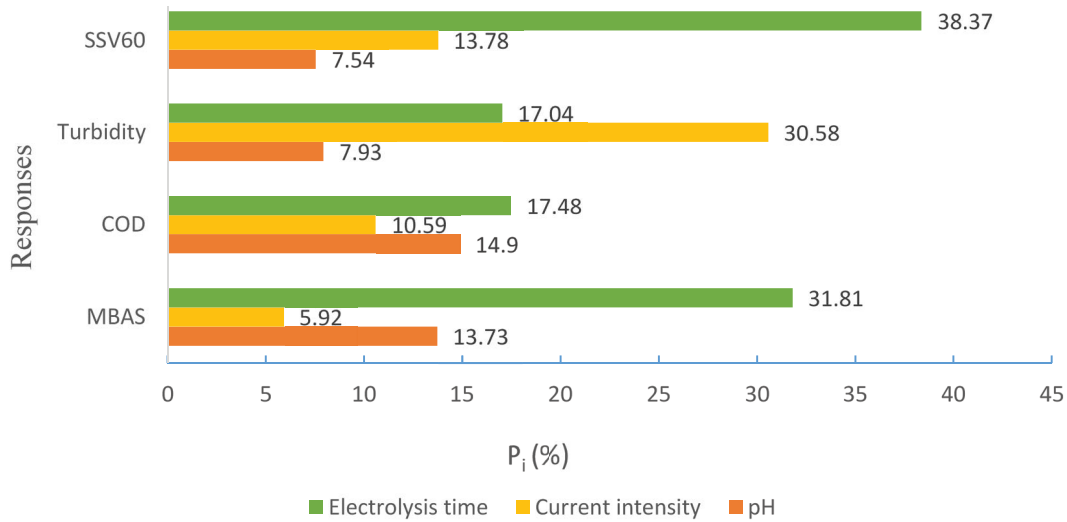
Fig. 5. Pareto analysis of the effects of factors on target responses for CCW treatment by ECF process.
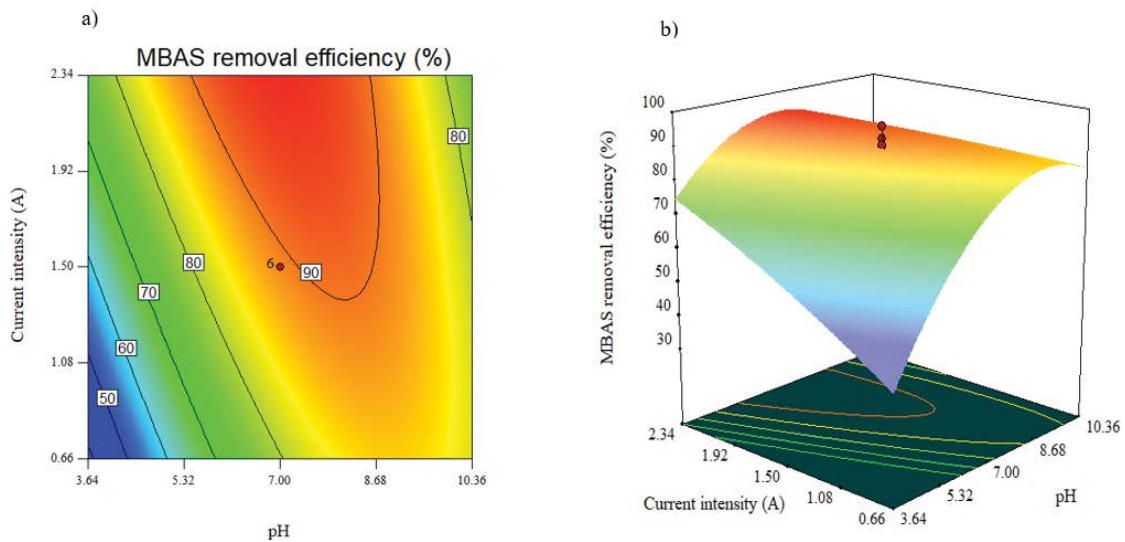
Fig. 6. 2D contours and 3D plot for the removal of MBAS: the effect of current intensity and initial pH (constant electrolysis time of 60 min).

reduction (~90%) was fast and realized within 15 min and leveled off at the extended operation times. The responsible COD removal mechanism was explained as electrochemical oxidation and adsorption by electrostatic attraction and physical entrapment [24]. In another study performed using a laundry effluent, 92.8% COD and 89.2% turbidity removals were attained by EC/EF process with aluminum electrodes operated under the optimum conditions (current density: 12.82 mA/cm² (1.5 A), initial pH: 5, electrolysis time: 5 min) [50]. Moreover, Wang et al. [52] investigated COD removal from simulated laundry wastewater by electrocoagulation/electroflotation process. Their results demonstrated that the extension of electrolysis time from 10 to 40 min resulted in an increase in COD removal efficiency from 20.8% to 53.5%. These literature data revealed that longer electrolysis times were required to attain reasonable COD removal efficiencies such as higher than 90% in the present study conditions.

4.4. Turbidity removal efficiency

Fig. 8 displays the effect of electrolysis time and current intensity on turbidity removal efficiency as 2D contours (a) and 3D plot (b), while another factor was fixed at the center point (initial pH of 7). As can be inferred from the figures, as the electrolysis time and current intensity increased, the turbidity decreased and a further rise in electrolysis time to 100 min and current intensity to 2 A caused a decrease in turbidity removal efficiency. It could be attributed to the accelerated production of coagulants with the increment in both the factors of electrolysis time and current intensity, thus resulting in an improvement in the removal efficiency of the target pollutant [54,55]. Findings from previous works [56–58] are well in line with this deduction. As both long electrolysis time and high current intensity are not cost-effective for an electrocoagulation process due to the

Table 6
Comparison with the literature

Type of wastewater	Technique	Pollutant	Removal (%)	Operating cost	Reference
Carwash wastewater	EC (Al)	COD	88	0.3 US$/m³	Gonder et al. [49]
		Oil & grease	68		
		Chloride	33		
Carwash wastewater	EC (Fe)	COD	88	0.6 US$/m³	Gonder et al. [49]
		Oil & grease	90		
		Chloride	50		
Carwash wastewater	ECF+	COD	94.5	0.23 US$/m³	Emamjomeh et al. [26]
	Sedimentation+	MBAS	95.2		
	Filtration	Turbidity	95		
Laundry wastewater	ECF (Al)	COD	92.8	–	Yazd et al. [50]
		Phosphate	98.6		
		Turbidity	89.2		
Laundry wastewater	ECF (Al)	COD	93.2	–	Janpoor et al. [51]
		Phosphate	96.7		
		Detergent	93.5		
		Color	90.1		
		Turbidity	95.9		
Laundry wastewater	ECF (Al)	COD	53.5	–	Wang et al. [52]
Carpet cleaning wastewater	ECF (Al)	MBAS	85.5	0.673 US$/m³	Present study
		COD	84.4		
		Turbidity	90.5		
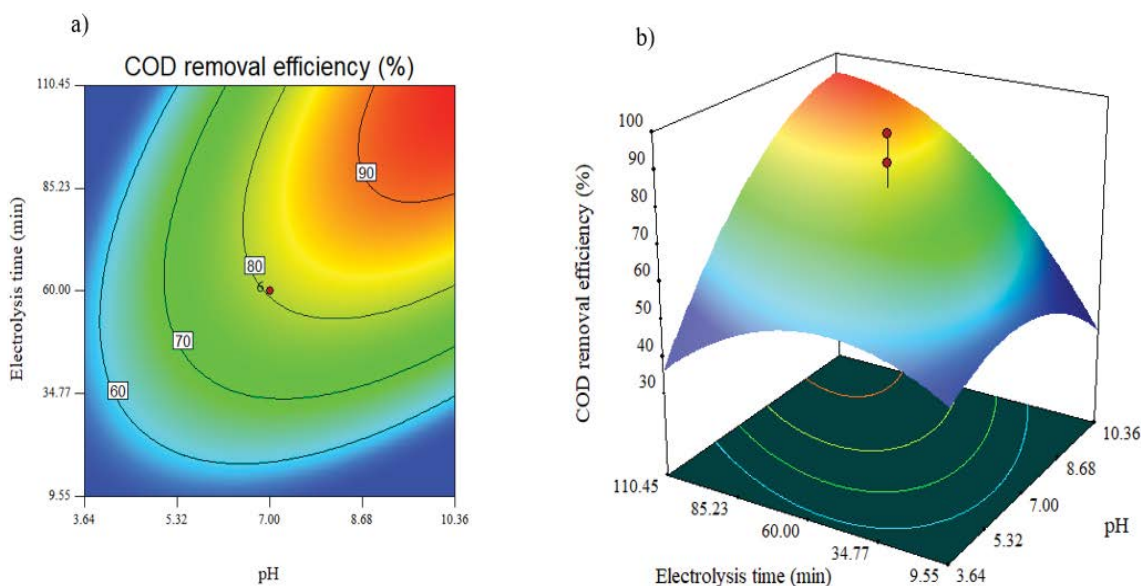
Fig. 7. 2D contours and 3D plot for the removal of COD: the effect of electrolysis time and pH (constant current intensity of 1.5 A).

increase in both energy and electrode consumption. It was worth pointing out that the highest turbidity removal rate as 98.75%, was observed at neutral pH, high current intensity (2.34 A), and electrolysis time of 60 min. These conclusions were in complete contrast with the recent scientific literature [24,50]. In the present study, aluminum electrodes were preferred instead of iron electrodes because the iron electrode prompted an additional color in the effluent owing to its chemical characteristics, thus leading to additional turbidity in the effluent of the ECF process. The formation of colored effluent after the ECF process could be attributed to the high concentration of residual [57,59].

Based on the literature, the removal of turbidity from marble processing wastewaters by aluminum-electrocoagulation

process at the beginning of the process (after 1 min) resulted in a very high efficiency of 99% [60]. Adamovic et al. [19] revealed that higher current density contributes to a significant increase in removal efficiency and shorter the ECF process. This is due to the fact that more amount of precipitate is created as a result of the anodic dissolution of electrodes at high current densities to remove contaminants. In former studies [19,61], can be seen similar results which accord with our conclusion.

4.5. Settled sludge volume

Figs. 9a and b depict the interaction of the current intensity and pH on the SSV_{60}. As expected, unsatisfactorily sludge formation was observed during the ECF applications initiated at the acidic pH values and imposed the current intensity less than 1.5 A. Increasing the current intensity up to 2 A and initial pH values to 7.5 promoted sludge production during the process and at the end of these ECF runs, SSV_{60} values varied between 50.13 and 420.33 mL/L. Low SSV_{60} values due to low flocs formation indicating poor settling character were obtained at higher current densities (>2 A) and initial alkaline pH values. It is not unexpected to observe such an effect in the case of ECF operations initiated at alkaline pH values since the solubility of $Al(OH)_3$ drastically increases due to the formation of $Al(OH)_4^-$. Although sludge settling characteristics in terms of SVI as well as sludge formation rate significantly enhances with increasing the applied current density [62], a negative effect of the current density on SSV was observed in the present study. The deterioration on sludge settling characteristics could be explained by the improvement in simultaneous flotation of $Al(OH)_3$ via hydrogen bubbles formed at the cathode since the hydrogen gas bubble size decreased with increasing the current density [63].
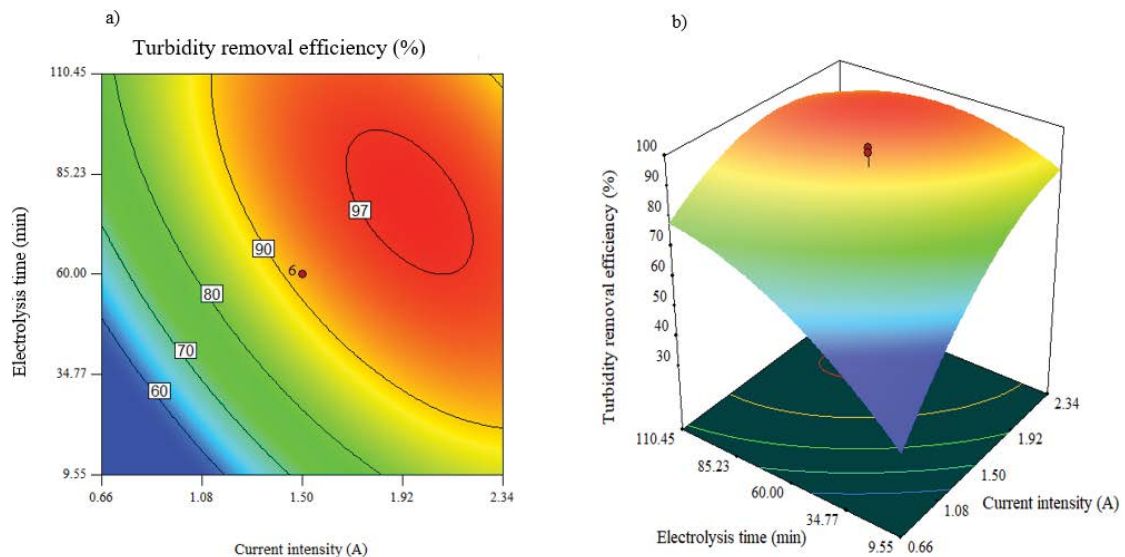
Fig. 8. 2D contours and 3D plot for the removal of turbidity: the effect of electrolysis time and current intensity (constant initial pH 7).
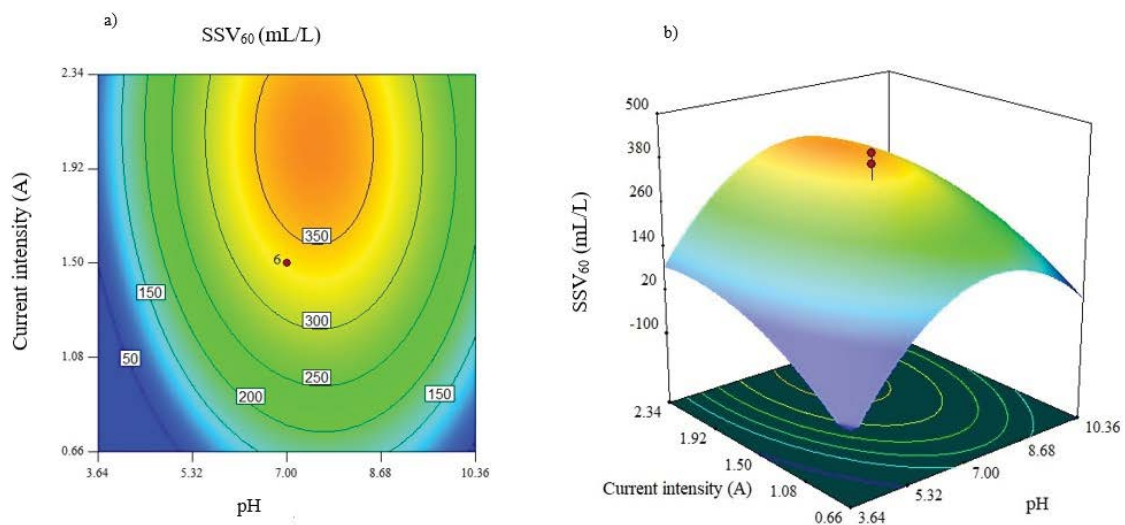
Fig. 9. 2D contours and 3D plot for the removal of SSV: the effect of current intensity and pH (constant electrolysis time of 60 min).

Sinha et al. [64] investigated fluoride removal from aqueous solution by EC with aluminum electrodes and targeted to reduce the content of aluminum remaining lower than 0.2 mg/L recommended by the World Health Organization in the effluent. To improve the effluent quality in terms of residual aluminum as well as sludge settling characteristic, two treatment alternatives were tested. The first alternative was to continue the stirring for 20 min to promote floc formation after the EC process and then settling, followed by filtration. SSV was obtained as 150 mL/L for this alternative. After the EC process, the addition of bentonite clay as a cheap coagulation aid was the second alternative tested in their study. Bentonite clay improved the settling characteristic yielding SSV of 120 mL/L. They proposed bentonite clay added coagulation and settling alternative since its addition did not affect the effluent character and compressed the sludge volume, and made the sludge handling process easier. Bakshi et al. [54] modelled phosphate removal from aqueous solution by EC utilizing scrap aluminum plate electrode. Agitation (50–290 rpm) was applied to the EC treated effluents for 5 min to obtain clear supernatant. They reported that SSV of 120 and 125 mL/L yielded the clearest supernatant, and an agitation speed of 110 rpm and a duration of 90 min could be considered as optimum conditions to design the settling tank. Hence, several EC operating parameters such as initial and effluent pH, current intensity, and electrolysis time influence the sludge settling character. As it turns out, plain settling is not a proper way to separate produced sludge after the ECF process with aluminum electrodes, increase agitation speed and duration, changing the type of electrodes, applying filtration rather than settling, and addition of auxiliary coagulants such as bentonite clay seem to be good solutions to overcome this drawback.

4.6. Optimization process and cost-effectiveness estimation

The RSM-CCD also devotes the optimization of operating conditions for maximum MBAS, COD, and turbidity removal efficiencies as well as SSV_{60}. The output of the results revealed that the optimal variables are comprised of initial pH of 5.1, current intensity of 2 A, and electrolysis time of 53.5 min. As per the model predictions, the highest removal efficiencies for MBAS, COD, turbidity, and SSV_{60} are achieved 83.56%, 82.54%, 88.14%, and 226.22 mL/L, respectively. Thus, a number of assays were performed under the optimum conditions in order to verify the model prediction. The targeted responses close to the predicted values (85.50%, 84.35%, 90.50%, and 240.17 mL/L, respectively). The actual results for response factors denote a realistic predictive model. According to Eqs. (11) and (12), the amount of electrodes material and energy consumed were calculated to estimate the operating cost of ECF as Eq. (10). Under optimal conditions, the energy consumed, the electrode mass-consumed material, and the operating cost were achieved as 0.356 kWh/m^3, 0.331 kg Al/m^3, and 0.673 USD/m^3.

5. Conclusions

In the present, the CCD coupled with RSM was applied to model and optimize operation parameters in the ECF

treatment of the CCW. MBAS, COD, and turbidity, as well as SSV_{60} as target responses and the other side pH, current intensity, and electrolysis time as independent variables were modeled using RSM-CCD. The effects of independent variables and their interactions on process performance were investigated by means of 2D contours and a 3D plot. The following conclusions could be drawn from the present study.

- The electrocoagulation–flocculation followed sedimentation proved to be a feasible and cost-effective process for the treatment of the carpet cleaning wastewater.
- The ANOVA results indicated that the best model obtained using the CCD were quadratic polynomial for MBAS and turbidity removals (0.93 and 0.94, respectively).
- The Pareto analysis revealed that the factor of electrolysis time had the highest percent contribution as 31.81%, 17.48%, and 38.37% for MBAS and COD removal efficiencies and SSV_{60}, respectively, while the factor of initial pH did not influence noticeably on the responses as contributed to 5.92%, 7.93%, and 7.54%, for MBAS and turbidity removal efficiencies, and SSV_{60}, respectively.
- For the optimum operation conditions determined as an initial pH of 5.1, a current intensity of 2A, and an electrolysis time of 53.5 min, the model predictions were in good agreement with the experimental data.
- The operation cost in the optimum conditions was calculated as 0.673 USD/m^3.

Although reasonable SSV_{60} values could be achieved by subsequent plain settling, the settling characteristics could be improved by adjusting the effluent pH to the optimum pH of $Al(OH)_3$ to precipitate residual aluminum or using subsequent filtration or bentonite clay added coagulation.

References

[1] F. Changani, A. Asadi, G.A. Haghighat, A.H. Mahvi, Characterization of carpet cleaning wastewater in Tehran, Iran, Iran. J. Health Environ., 5 (2012) 99–106.
[2] M.C. Collivignarelli, M.C. Miino, M. Baldi, S. Manzi, A. Abbà, G. Bertanza, Removal of non-ionic and anionic surfactants from real laundry wastewater by means of a full-scale treatment system, Process Saf. Environ. Prot., 132 (2019) 105–115.
[3] C. Ramprasad, L. Philip, Surfactants and personal care products removal in pilot scale horizontal and vertical flow constructed wetlands while treating greywater, Chem. Eng. J., 284 (2016) 458–468.
[4] M. Palmer, H. Hatley, The role of surfactants in wastewater treatment: impact, removal and future techniques: a critical review, Water Res., 147 (2018) 60–72.
[5] J. Sun, X. Li, J. Feng, X. Tian, Oxone/Co^{2+} oxidation as an advanced oxidation process: comparison with traditional Fenton oxidation for treatment of landfill leachate, Water Res., 43 (2009) 4363–4369.
[6] S. Saroj, S.V. Singh, D. Mohan, Removal of colour (Direct Blue 199) from carpet industry wastewater using different biosorbents (Maize Cob, Citrus Peel and Rice Husk), Arabian J. Sci. Eng., 40 (2015) 1553–1564.

[7] M. Moradnia, K. Dindarlo, H.A. Jamali, Optimizing potassium ferrate for textile wastewater treatment by RSM, Environ. Eng. Manage. J., 3 (2016) 137–142.

[8] J. Jaafari, A.B. Javid, H. Barzanouni, A. Younesi, N. Amir, A. Farahani, M. Mousazadeh, P. Soleimanie, Performance of modified one-stage Phoredox reactor with hydraulic up-flow in biological removal of phosphorus from municipal wastewater, Desal. Water Treat, 171 (2019) 216–222.

[9] G. Singh, S. Dwivedi, Decolorization and degradation of Direct Blue-1 (Azo dye) by newly isolated fungus *Aspergillus terreus* GS28, from sludge of carpet industry, Environ. Technol. Innovation, 18 (2020) 100751, doi: 10.1016/j.eti.2020.100751.

[10] M.M. Emamjomeh, H. Torabi, M. Mousazadeh, M.H. Alijani, F. Gohari, Impact of independent and non-independent parameters on various elements' rejection by nanofiltration employed in groundwater treatment, Appl. Water Sci., 9 (2019) 71, doi: 10.1007/s13201-019-0949-1.

[11] J. Lakshmi, G. Sozhan, S. Vasudevan, Recovery of hydrogen and removal of nitrate from water by electrocoagulation process, Environ. Sci. Pollut. Res., 20 (2013) 2184–2192.

[12] M.Y.A. Mollah, R. Schennach, J.R. Parga, D.L. Cocke, Electrocoagulation (EC)—science and applications, J. Hazard. Mater., 84 (2001) 29–41.

[13] F. Özyonar, M. Karagozoglu, Removal of turbidity from drinking water by electrocoagulation and chemical coagulation, J. Fac. Eng. Archit. Gazi Univ., 27 (2012) 81–89.

[14] M. Arroyo, V. Pérez-Herranz, M. Montanes, J. García-Antón, J. Guinon, Effect of pH and chloride concentration on the removal of hexavalent chromium in a batch electrocoagulation reactor, J. Hazard. Mater., 169 (2009) 1127–1133.

[15] E. Nazlabadi, M.A. Alavi Moghaddam, Simulation of nitrate removal in a batch flow electrocoagulation–flotation (ECF) process by response surface method (RSM), F. Kurisu, A. Ramanathan, A. Kazmi, M. Kumar, Eds., Trends in Asian Water Environmental Science and Technology, Springer, Cham, 2017, pp. 49–60.

[16] F. Ozyonar, B. Karagozoglu, Operating cost analysis and treatment of domestic wastewater by electrocoagulation using aluminum electrodes, Pol. J. Environ. Stud., 20 (2011) 173–179.

[17] F. Ghanbari, M. Moradi, A. Eslami, M.M. Emamjomeh, Electrocoagulation/flotation of textile wastewater with simultaneous application of aluminum and iron as anode, Environ. Process., 1 (2014) 447–457.

[18] F. Ozyonar, Optimization of operational parameters of electrocoagulation process for real textile wastewater treatment using Taguchi experimental design method, Desal. Water Treat., 57 (2016) 2389–2399.

[19] S. Adamovic, M. Prica, B. Dalmacija, S. Rapajic, D. Novakovic, Z. Pavlovic, S. Maletic, Feasibility of electrocoagulation/flotation treatment of waste offset printing developer based on the response surface analysis, Arabian J. Chem., 9 (2016) 152–162.

[20] M. Elazzouzi, K. Haboubi, M. Elyoubi, Enhancement of electrocoagulation-flotation process for urban wastewater treatment using Al and Fe electrodes: techno-economic study, Mater. Today:. Proc., 13 (2019) 549–555.

[21] M. Prica, S. Adamovic, B. Dalmacija, L. Rajic, J. Trickovic, S. Rapajic, M. Becelic-Tomin, The electrocoagulation/flotation study: the removal of heavy metals from the waste fountain solution, Process Saf. Environ. Prot., 94 (2015) 262–273.

[22] B. Khaled, B. Wided, H. Béchir, E. Elimame, L. Mouna, T. Zied, Investigation of electrocoagulation reactor design parameters effect on the removal of cadmium from synthetic and phosphate industrial wastewater, Arabian J. Chem., 12 (2019) 1848–1859.

[23] I. Linares-Hernández, C. Barrera-Díaz, G. Roa-Morales, B. Bilyeu, F. Ureña-Núñez, Influence of the anodic material on electrocoagulation performance, Chem. Eng. J., 148 (2009) 97–105.

[24] F. Janpoor, A. Torabian, V. Khatibikamal, Treatment of laundry waste-water by electrocoagulation, J. Chem. Technol. Biotechnol., 86 (2011) 1113–1120.

[25] M.M. Emamjomeh, M. Mousazadeh, N. Mokhtari, H.A. Jamali, M. Makkiabadi, Z. Naghdali, K.S. Hashim, R. Ghanbari, Simultaneous removal of phenol and linear alkylbenzene sulfonate from automotive service station wastewater: optimization of coupled electrochemical and physical processes, Sep. Sci. Technol., 55 (2020) 3184–3194.

[26] M.M. Emamjomeh, H.A. Jamali, Z. Naghdali, M. Mousazadeh, Carwash wastewater treatment by the application of an environmentally friendly hybrid system: an experimental design approach, Desal. Water Treat., 160 (2019) 171–177.

[27] E.B. Butler, Y.T. Hung, O. Mulamba, The effects of chemical coagulants on the decolorization of dyes by electrocoagulation using response surface methodology (RSM), Appl. Water Sci., 7 (2017) 2357–2371.

[28] F. Doosti, R. Ghanbari, HA. Jamali, H. Karyab, Optimizing fenton process for olive mill wastewater treatment using response surface methodology, Fresenius Environ. Bull., 26 (2017) 5942–5953.

[29] M. Behbahani, M. Alavi Moghaddam, M. Arami, Phosphate removal by electrocoagulation process: optimization through response surface methodology, Environ. Eng. Manage. J., 12 (2013) 2397–2405.

[30] D.-S. Kim, Y.S. Park, Application of the central composite design and response surface methodology to the treatment of dye using electrocoagulation/flotation process, J. Korean Soc. Water Environ., 26 (2010) 35–43.

[31] S.S. Moghaddam, M.A. Moghaddam, M. Arami, Coagulation/flocculation process for dye removal using sludge from water treatment plant: optimization through response surface methodology, J. Hazard. Mater., 175 (2010) 651–657.

[32] M. Taheri, M.A. Moghaddam, M. Arami, Techno-economical optimization of Reactive Blue 19 removal by combined electrocoagulation/coagulation process through MOPSO using RSM and ANFIS models, J. Environ. Manage., 128 (2013) 798–806.

[33] A.G. Khorram, N. Fallah, Treatment of textile dyeing factory wastewater by electrocoagulation with low sludge settling time: optimization of operating parameters by RSM, J. Environ. Chem. Eng., 6 (2018) 635–642.

[34] Ş. İrdemez, N. Demircioğlu, Y.Ş. Yıldız, Z. Bingül, The effects of current density and phosphate concentration on phosphate removal from wastewater by electrocoagulation using aluminum and iron plate electrodes, Sep. Purif. Technol., 52 (2006) 218–223.

[35] B. Abdulhadi, P. Kot, K. Hashim, A. Shaw, M. Muradov, R. Al-Khaddar, Continuous-flow electrocoagulation (EC) process for iron removal from water: experimental, statistical and economic study, Sci. Total Environ., 760 (2020) 143417, doi: 10.1016/j.scitotenv.2020.143417.

[36] M.A. Zazouli, J. Yazdani Charati, M. Alavinia, Y. Esfandyari, Efficiency of electrocoagulation process using aluminum electrode in hospital laundry wastewater pretreatment, J. Mazandaran Univ. Med. Sci., 25 (2016) 251–260.

[37] APHA, AWWA, WEF, Standard Methods for the Examination of Water and Wastewater, 2nd ed., American Public Health Association, American Water Works Association, Water Pollution Control Federation, Water Environment Federation, New York, 2003.

[38] S. Chitikela, S.K. Dentel, H.E. Allen, Modified method for the analysis of anionic surfactants as methylene blue active substances, Analyst, 120 (1995) 2001–2004.

[39] APHA, AWWA, WEF, Standard Method for Examination of Water and Wastewater, American Public Health Association, American Water Works Association, Water Pollution Control Federation, Water Environment Federation, Washington, DC, USA, 2005.

[40] S. Abbasi, M. Mirghorayshi, S. Zinadini, A. Zinatizadeh, A novel single continuous electrocoagulation process for treatment of licorice processing wastewater: optimization of operating factors using RSM, Process Saf. Environ. Prot., 134 (2020) 323–332.

[41] M. Abdulgader, J. Yu, A.A. Zinatizadeh, P. Williams, Z. Rahimi, Process analysis and optimization of single stage flexible fibre biofilm reactor treating milk processing industrial wastewater using response surface methodology (RSM), Chem. Eng. Res. Des., 149 (2019) 169–181.

[42] M.M. Emamjomeh, S. Kakavand, H.A. Jamali, S.M. Alizadeh, M. Safdari, S.E.S. Mousavi, K.S. Hashim, M. Mousazadeh, The treatment of printing and packaging wastewater by electrocoagulation–flotation: the simultaneous efficacy of critical parameters and economics, Desal. Water Treat., 205 (2020) 161–174.

[43] W. Yassine, S. Akazdam, S. Zyade, B. Gourich, Treatment of olive mill wastewater using electrocoagulation process, J. Appl. Surf. Interfaces, 4 (2018), doi: 10.48442/IMIST.PRSM/jasi-v4i1-3.14006.

[44] Z. Naghdali, S. Sahebi, R. Ghanbari, M. Mousazadeh, H.A. Jamali, Chromium removal and water recycling from electroplating wastewater through direct osmosis: modeling and optimization by response surface methodology, Environ. Eng. Manage. J., 6 (2019) 113–120.

[45] Z.B. Gönder, S. Arayici, H. Barlas, Treatment of pulp and paper mill wastewater using utrafiltration process: optimization of the fouling and rejections, Ind. Eng. Chem. Res., 51 (2012) 6184–6195.

[46] S. Barışçı, O. Turkay, Domestic greywater treatment by electrocoagulation using hybrid electrode combinations, J. Water Process Eng., 10 (2016) 56–66.

[47] A. Dimoglo, P. Sevim-Elibol, Ö. Dinç, K. Gökmen, H. Erdoğan, Electrocoagulation/electroflotation as a combined process for the laundry wastewater purification and reuse, J. Water Process Eng., 31 (2019) 100877, doi: 10.1016/j.jwpe.2019.100877.

[48] B. Mohebrad, A. Rezaee, S. Dehghani, Anionic surfactant removal using electrochemical process: effect of electrode materials and energy consumption, Iran. J. Health Saf. Environ., 5 (2018) 939–946.

[49] Z.B. Gonder, G. Balcioglu, I. Vergili, Y. Kaya, Electrochemical treatment of carwash wastewater using Fe and Al electrode: techno-economic analysis and sludge characterization, J. Environ. Manage., 200 (2017) 380–390.

[50] M. Yazd, B. Aminzadeh, A. Torabian, Laundry wastewater treatment using electrocoagulation/flotation and electro-Fenton processes, J. Environ. Stud., 39 (2013) 1–2.

[51] F. Janpoor, A. Torabian, V. Khatibikamal, Treatment of laundry waste-water by electrocoagulation, J. Chem. Technol. Biotechnol., 86 (2011) 1113–1120.

[52] C.T. Wang, W.L. Chou, Y.M. Kuo, Removal of COD from laundry wastewater by electrocoagulation/electroflotation, J. Hazard. Mater., 164 (2009) 81–86.

[53] Ö. Kahraman, İ. Şimşek, Color removal from denim production facility wastewater by electrochemical treatment process and optimization with regression method, J. Cleaner Prod., 267 (2020) 122168, doi: 10.1016/j.jclepro.2020.122168.

[54] A. Bakshi, A.K. Verma, A.K. Dash, Electrocoagulation for removal of phosphate from aqueous solution: Statistical modeling and techno-economic study, J. Cleaner Prod., 246 (2020) 118988, doi: 10.1016/j.jclepro.2019.118988.

[55] V. Kuokkanen, T. Kuokkanen, J. Rämö, U. Lassi, J. Roininen, Removal of phosphate from wastewaters for further utilization using electrocoagulation with hybrid electrodes–techno-economic studies, J. Water Process Eng., 8 (2015) e50–e57.

[56] R. Niazmand, M. Jahani, F. Sabbagh, S. Rezania, Optimization of electrocoagulation conditions for the purification of table olive debittering wastewater using response surface methodology, Water, 12 (2020) 1687, doi: 10.3390/w12061687.

[57] F. Ozyonar, B. Karagozoglu, Systematic assessment of electrocoagulation for the treatment of marble processing wastewater, Int. J. Environ. Sci. Technol., 9 (2012) 637–646.

[58] R. Sridhar, V. Sivakumar, J.P. Maran, K. Thirugnanasambandham, Influence of operating parameters on treatment of egg processing effluent by electrocoagulation process, Int. J. Environ. Sci. Technol., 11 (2014) 1619–1630.

[59] M. Kobya, H. Hiz, E. Senturk, C. Aydiner, E. Demirbas, Treatment of potato chips manufacturing wastewater by electrocoagulation, Desalination, 190 (2006) 201–211.

[60] M. Solak, M. Kılıç, Y. Hüseyin, A. Şencan, Removal of suspended solids and turbidity from marble processing wastewaters by electrocoagulation: comparison of electrode materials and electrode connection systems, J. Hazard. Mater., 172 (2009) 345–352.

[61] B. Merzouk, B. Gourich, A. Sekki, K. Madani, M. Chibane, Removal turbidity and separation of heavy metals using electrocoagulation–electroflotation technique: a case study, J. Hazard. Mater., 164 (2009) 215–222.

[62] I. Kabdaşlı, T. Arslan, T. Ölmez-Hanci, I. Arslan-Alaton, O. Tünay, Complexing agent and heavy metal removals from metal plating effluent by electrocoagulation with stainless steel electrodes, J. Hazard. Mater., 165 (2009) 838–845.

[63] A.G. Khorram, N. Fallah, Comparison of sludge settling velocity and filtration time after electrocoagulation process in treating industrial textile dyeing wastewater: RSM optimization, Int. J. Environ. Sci. Technol., 16 (2019) 3437–3446.

[64] R. Sinha, S. Mathur, U. Brighu, Aluminum removal from water after defluoridation with the electrocoagulation process, Environ. Technol., 36 (2015) 2724–2731.